Int. J. Electrochem. Sci., 17 **(2022)** Article Number: 220512, doi: 10.20964/2022.05.25

International Journal of
ELECTROCHEMICAL
SCIENCE
www.electrochemsci.org

Voltammetric Behaviour of an Electroactive of Zn^{2+} - octa(aminopropyl)silsesquioxane nanocoposite : An Application to 4-Chlorophenol Detection in Tap Water

Fernanda dos Santos Franco[1], Murilo Santos Peixoto[1], Abner Santos Baroni[1], Alexsandro dos Santos Felipe[2], Priscila Fernanda Pereira Barbosa[1], Vitor Alexandre Maraldi[1], Rebeca Moreira Lima Freitas[2], Stefani Fernanda Vicente Da Silva[1], Vanessa Petronília Alves[2], Alvaro Adriano Couto Moraes[2], Idalci Cruvinel dos Reis[2], Devaney Ribeiro do Carmo[1,]*

[1] Faculdade de Engenharia de Ilha Solteira, Universidade Estadual Paulista "Júlio de Mesquita Filho", Departamento de Física e Química, Av. Brasil, 56, ZIP-code 15385-000, Ilha Solteira-SP, Brazil.
[2] Instituto Federal Goiano. Nanostructured Materials Laboratory, Rodovia Sul Goiana, Km 01, Zona Rural, Rio Verde, Go CEP: 75.901-970 Brazil.
[*]E-mail: devaneydocarmo@hotmail.com

Received: 7 January 2021 / *Accepted:* 23 February 2022 / *Published:* 5 April 2022

This paper presents the voltammetric behavior of electroactive metallosilsesquioxane and their use in the detection of 4-CP. The metallosilsesquioxane was synthesized in two steps. First by direct reaction between hydrochloride octa(aminopropyl)silsesquioxane (POSS-$NH_3^+Cl^-$) and Zn^{2+} a second by electrostatic interaction with $[FeCN_6]^{4-}$ (SZnFe). The nanostructured material showed a well-defined three redox couples with formal potential ($E^{0'}$) of approximately 0.33, 0.78 and 1.01 ± 0.01V (*vs* Ag/AgCl). Voltammetric analysis showed that the formal potential ($E^{0'}$) strongly depends on concentration and electrolyte type, but the system remained unchanged with pH values between 2 and 8. The SZnH graphite paste electrode exhibits a sensitive and catalytic oxidation response for the detection of 4-CP. For detection of 4-CP, the modified graphite paste electrode had a linear range of 6.0×10^{-7} to 6.0×10^{-5} mol L^{-1} with a limit of detection of 5.3×10^{-6} mol L^{-1} and a sensitivity of 0.53 A/ mol L^{-1}. This electrode could be used to detect 4-CP in tap water.

Keywords: Metallosilsesquioxane; Octa(aminopropyl)silsesquioxane; Prussiam blue analogs; Voltammetry; Graphite Paste Electrode; 4-Chlorophenol.

1. INTRODUCTION

Research in advanced polymers, composites and nanostructured materials has collaborated to the development of new materials for technological application in recent years, constituting a research center that attracts researchers from other fields of knowledge.

Silsesquioxanes are nanostructured materials characterized by O-Si-O bonds and a general formula $(RSiO_{1.5})$ n, where R represents a hydrogen atom or an organic group [1,2]. These organic groups generally are used in grafting reactions or in polymerization and which can be easily functionalized using a large range of organic. Polyhedral oligomeric silsesquioxanes (POSS) have high thermal and oxidative stability, relative hardness and allow for a great variety of structures and pendant groups. Due to these properties these materials have attracted much attention in recent years, as models for efficient catalytic surfaces [3,4] and also to generate new catalysts and act as new encapsulants [5] POSS, also known as cubic silsesquioxanes that can be used as blocks of construction for nanocomposite materials [6-10]. A special interest of ours is highly symmetric cubic silsesquioxanes, which are unique spherical organic/inorganic molecules consisting of rigid silica cores with eight vertices (vertex body diagonal = 0.53 nm) and each including an organic portion [11] that is susceptible to diverse chemical reactions. They are 1-2 nm in diameter with volumes < 2 nm^3 [11]. The general interest of researchers in organic- inorganic hybrid materials has led to the development of many routes for the preparation of materials based on organic polymers, incorporating inorganic building blocks at the nanoscale.

In the area of polyhedral silsesquioxane chemistry, there has been a noticeable increase in activity due to the growth in interest in coordination polymers. Most syntheses of metallic cubic silsesquioxanes are carried out starting from open chain precursors, using corner capping reactions, eg trisilanol POSS with titanium alkoxide [12,13]. The possibility of producing metallic cubic silsesquioxanes directly and with good yields opens up excellent prospects for their use as catalysts and electrocatalysts.

In this context, the present work, hydrochloride octa (aminopropyl) silsesquioxane was prepared and chemically modified with electroactive mixed valence complexes from the direct chemical reaction of a POSS salt $(Si_8O_{12}[(CH_2)_3NH_3^+Cl^-]_8$ with Zn^{2+} and sub- sequent reac- tion of $[Fe(CN)_6]^{4-}$ ions. Some Zn-POSS structures have already been reported by Hanssen [44], in this case he used corner capping reactions [14].

Direct reaction of $[SiO1.5\ (CH_2)_3NH_3)]_8Cl_8$ with Co(II), Cu(II) and Cd(II) chlorides in methanol gave the compounds $[SiO1.5(CH_2)_3NH_3)]_8{}^{8+}$. $4[MCl_4]^{-2}$ $[Si_8O_{12}((CH_2)_3NH_3)_8][MCl_4]_4$ (M = Co, Cu, Cd) have been reported, by Goodgame [15] . Although these materials have been perfectly characterized, no practical application has been proposed by Gogname for these new metallic silsesquioxanes.

The Zn^{2+} was chosed because it is a lewis acid and its interactions are predomi- nantly ionic due and these properties should facilitate the interaction with basic sites of $[Si_8O_{12}((CH_2)_3NH_3)_8]Cl_8$ and can suffer subsequently reaction with electroactive $[Fe(CN)_6]^{4-}$ anion to forme POSS-composite (SZnH).The electrochemical behavior of the SZnH formed was studied in presence of 4-CP. 4-CP is a pesticide and biocide precursor, and is also used in the most diverse industrial activities including: bleaching of cellulose pulp in the paper industry, drug preparation and is present in gas residues and industrial oils, it is also used mainly in the cultures of cereals, sorghum, rice and mainly sugar cane. Phenolic compounds with one or more aromatic rings, including 4-chloro-phenol (4-CP), are largely used for a wide variety of industrial applications (insecticides, herbicides, fungicides, dyes, and disinfectants). 4-CP is considered a highly toxic pollutant that has dangerous effects on the environment as well as on humans [16] The permissible limit in natural waters is 100 $\mu g\ L^{-1}$, according to the "US Environmental Protection Agency"4 (EPA) but according to the European Community (EC), the allowed

level of phenols in wastewater is about 1ppm [17-20]. Several techniques have been used to determine 4-CP; among them, gas chromatography (GC) and high performance liquid chromatography (HPLC) are widely used methods, but they suffer from bulky instruments and cumbersome sample preparation [21,22].

As most electroanalytical studies for the determination of pesticides were carried out on the mercury electrode, which is an extremely toxic material, the awareness of its high danger leads to the search for new materials. Using electrochemical techniques, most sensors reported use polymers, expensive metal electrodes (Au, Pd etc.) or hybrid materials [23–31]. However, no report was found on the electroanalytical determination of 4-CP using the silsesquioxane proposed in this project.

2. EXPERIMENTAL

2.1. Reagents and solutions

3-Aminopropyltriethoxysilane (APTES), Zinc chloride, potassium hexacyanoferrate (II), 4-Chlorophenol (4-CP), and solvents were of analytical grade and purchased from (Sigma- Aldrich, Alpha Aesar or Merck) and were used as received. All analytical solutions and supporting electrolytes were prepared from deionized water using reverse osmosis system.

2.2. Techniques

The previously prepared material (SZnH) was characterized by spectroscopic techniques, such infra-red (FTIR) and Scanning electron microscopy (SEM)coupled with Energy x-ray (EDX). The FTIR spectra were recorded on a Nicolet 5DXB FTIR spectrometer. About 150 mg of KBr were ground with a mortar and a sufficient amount of the solid sample was ground with the KBr to produce a 1 wt.% mixture resulting in pellets. Data collection comprised a minimum of 64 scans for each sample at a resolution of ± 4 cm^{-1} in the range of 4000 to 400 cm^{-1}. Scanning electron microscopy coupled with Energy-dispersive x-ray spectroscopy was obtained using a JEOL JSM T - 300 microscope. The samples were adhered over aluminum holders and covered with a thin layer of gold (20 - 30 nm) using a Tec SCD – 050 Sputter Coater Bal. Transmission electron microscopy analyses were performed using a Philips CM200 microscope equipped with a pole piece to obtain high-resolution images, operated at an accelerating voltage of 200 kV. The thermal analyses were carried out using an SDT Q600 thermal analyzer (TA Instruments). The sample analyses were performed ranging from room temperature up to 1000°C. Cyclic voltammograms were performed using a PGSTAT 128N Autolab potentiostat. The electrochemical measurements were performed using a computer controlled PalmSens3 potentiostat. A modified graphite paste electrode, a Pt wire and $Ag/AgCl_{(sat)}$) were used as working, counter electrode and reference electrode, respectively. The cyclic voltammetry was employed to study the detection of 4-CP (4-CP). In the voltammetric method, the analytical current was obtained by the difference between the current measured in the presence and absence of 4-CP.

2.4. Confection of chemically modified graphite paste electrodes

The SZnH-modified graphite paste electrode was developed in accordance with literature [13]. A study on the optimum composition of graphite and SZnH to be used for the detection of dopamine was carried out previously analyzing different compositions of paste (10, 20,30,40, 50% (w/w)), and 20% (w/w) was used for the preparation of the graphite paste electrode with SZnH.

2.5. Hydrochloride octa(aminopropyl)silsesquioxane (S) synthesis

The hydrochloride octa(aminopropyl)silsesquioxane (POSS-$NH_3^+Cl^-$) was developed according to a method reported in the literature [32] and scheme showed by Figure 1. Briefly, in a flat-bottomed 6000 mL flask equipped with a mechanical stirrer, containing 150 mL of 3-aminopropyltriethoxysilane ($H_2NCH_2CH_2CH_2Si(Oet)_3$) dissolved in 3.6 L of methanol, a concentrated HCl (200 mL) was slowly added. The homogeneous mixture was left for 6 weeks at room temperature. The hydrolysis and condensation step occurred for 6 weeks at room temperature and the crystalline precipitates were obtained as a result. The material was collected (3.7 g, 30% yield) after filtration, washed with methanol and dried in a vacum oven and for the sake of brevity, it was described as S.

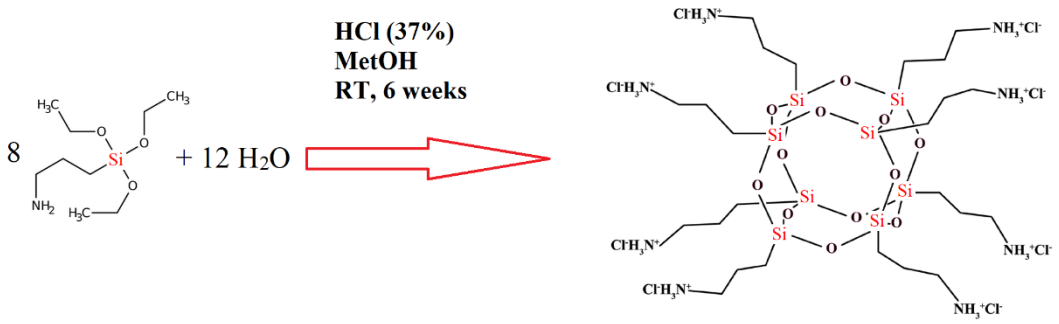

Figure 1. POSS-$NH_3^+Cl^-$ (S) preparation.

2.6. Preparation of Zn/ Fe complex

2.14 g of the S was dissolved in 60 mL of slightly heated methanol (40°C), then 1.09 g of $ZnCl_2$ dissolved in a minimal amount of slightly heated methanol was added and this solution was kept under stirring for 6 hours at room temperature. After this period 2.80 of potassium hexacyanoferrate ($K_4[Fe(CN)_6]$) was added to the previously prepared solution, this mixture was again stirred for 6 hours at room temperature. The precipitate obtained was carefully filtered, washed thoroughly with deionized water and dried at 80 ºC. The new formed hybrid composite present green color and was described as SZnH.

3. RESULTS AND DISCUSSION

The hydrochloride octa(aminopropyl)silsesquioxane (POSS-$NH_3^+Cl^-$) was synthesized via the γ-aminopropyltrimethoxysilane hydrolytic condensation in methanol under the catalytic action of concentrated hydrochloric acid. The amine hydrochloride, was prepared in 33–38% yield according to the method reported by Feher and co-workers [32] and shown in Figure 1 The precursor structures were initially characterized using vibrational spectroscopy The FTIR of the POSS-$NH_3^+Cl^-$, showed in Figure 2 (A), displayed the three absorption bands of primary amines: 3428 cm^{-1}, 1583 and 1505 relative to N-$H_{(\nu N-H)}$ stretching , deformation (N-$H_{(\delta N-H)}$) vibrations of NH_3^+ and NH_2 groups respectively; The other two bands at 2914 cm^{-1} and 1109 cm^{-1} were attributed to organic and CH_2 groups (C-$H_{(\nu C-H)}$) and axial symmetric stretching ((Si-O-Si)$_{(\nu Si-O-Si)}$,) where these bands are characteristic of the POSS-$NH_3^+Cl^-$ structure, as described in the literature [33,34]. Other absorption bands from 1048 to 806 cm^{-1} were assigned to special vibration feature of the silsesquioxane Si-O-Si cage structure. The absorption band at 1212 and 710 cm^{-1} relative to Si-$C_{(\nu Si-C)}$ stretching was assigned to the Si-C bond in $SiCH_2$. In addition, the stretching vibration of C-N is identified at 1242 cm^{-1} and those at 560 and 475 cm^{-1} are due to the deformation vibrations of POSS skeletal. Figure 2 (B) shows the spectrum in the infrared region for the SZnH, highlighting the most important vibrational modes The spectrum shows typical vibrations of its precursor S with lower intensities absorption, for example, at ~1110 cm^{-1} for the asymmetric stretching Si-O-$Si_{(\upsilon Si-O-Si)}$ deformation and NH_2 at 1486 cm^{-1} shifted 20 cm^{-1} toward to lower frequency and some vibrations which corresponds to the cage shaped structure of silsesquioxane. The bands at 3428 cm^{-1} and another intense band at 1610 cm^{-1}, attributed to symmetric N-H stretching and the angular N-H deformation are characteristic of primary amines. The broad adsorptive band at 3418 cm^{-1} corresponding to interstitial water or zeolitic water, which is result of water association due to the H-bonding. The presence of chloride ions in the composite was not clearly evidenced by XPS and EDX. By analogy, the composite could be represented for following expression. $[SiO_{1.5}(CH_2)_3NH_3)]_8^{8+}$. $4[ZnCl_4]^{-2}$.

After reaction of $[Fe(CN)_6]^{4-}$ some previous chloride ions present in the silsesquioxane structure have been exchanged for $[Fe(CN)_6]^{4-}$ ions, as showed by reaction above. When this occur a bimettalic complex is formed as suggested by equation (Eq. 1)

$$[SiO_{1.5}(CH_2)_3NH_3)]_8^{8+}.\ 4[ZnCl_4]^{-2} + 4[K_4\ Fe(CN)_6] \longrightarrow [SiO1.5(CH_2)_3NH_3)]_8^{8+}.\ 4\{[Zn[Fe(CN)_6]\}^{-2} + 16\ KCl \quad \text{(Eq. 1)}$$

The CN stretching vibration is sensitive to the coordination number for the zinc atom. The CN band frequency is a good sensor for the valance, electronic configuration and coordination number of the metals bonded at the C and N ends of the CN ligands. For C≡N vibration, the two bands at lower wavenumbers (2119 and 2161 cm^{-1}) are characteristics of cyanide stretching in reduced octahedrally coordinated iron-cyanide (Fe^{2+}–CN), while the single band at ca. 2191 cm^{-1} is characteristics of cyanide stretching near oxidized irons (Fe^{3+}–CN) [34,35].

The SZnH presents a strong peak around 2100 cm^{-1} ascribed to CN group (stretching ν_s (C≡N)) present in the moieties (Fe^{2+} –CN–Zn^{2+}). A shoulder absorption at 2162 cm^{-1} ascribed to free CN group was observed too. The observed peak at 491cm^{-1} corresponding to Zn–N group [35,36], In the high

frequency region, water molecules are associated with this complex, and a broad peak at 3631 cm^{-1} is associated to the presence of OH moiety from water molecules that were observed. Another peak at 1614 cm^{-1} is related to HOH bending. Lastly, peak at 602 cm^{-1}corresponds to Fe–C stretching [35]. These data confirmed the formation of a cyan-bridged network as demonstrated by the stretching displacement ν_s (C≡N) in relation to the potassium hexacyanoferrate (III) precursor (A).

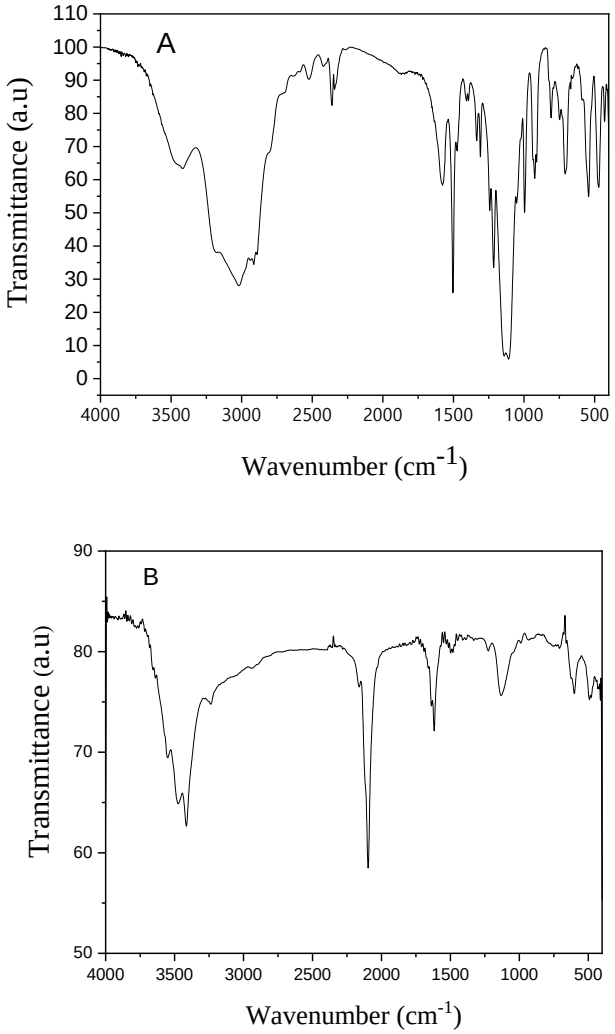

Figure 2. Vibrational spectra in the infrared region for (A) S, (B) SZnH.

In order to evaluate the catalytic properties of graphite paste electrode with SZnH (GPSZnH) to the detection of 4-CP, a preliminary voltammetric study was performed. Cyclic voltammetry is a powerful tool for investigating the properties of the modified interface and was the first technique applied herein. Figure 3 displays the voltammetric profile of graphite paste electrode with SZnH (GPZnH) previously manufactured. A Three process with formal potential ($E^{o'}$) of approximately 0.33, 0.78 and 1.01 ± 0.01V (*vs* Ag/AgCl) were observed, where $E^{o'} = (Ea_p + Ec_p)/2$ and Ea_p and Ec_p = anodic and cathodic peak potential respectively.

The presence of a third peak is probably related to the oxidation of part of the oxidized ferrocyanide ion in the reaction medium during synthesis. The presence of Fe^{3+} is in agreement with the data revealed by the XPS data. According to the scan rate studies, the third process moves to cathodic regions and from the scan rate of 200 mVs^{-1}, this redox process III practically disappears, while the first process shifts more smoothly to the cathodic regions; Process II, on the other hand, moves to the anodic regions.

For analytical studies, the redox process II was chosen due to its excellent performance and electrochemical stability and ease of obtaining catalytic currents,

To estimate the effective surface area of the electrode containing S, using the Randles-Sevcik equation (Eq. 2), the electrode containing S was immersed in 10 mM potassium ferricyanide and 0.5 mol L^{-1} KCl [37]

$$I_p = (2.69\times10^5)n^{2/3}A\ .D^{1/2}CV^{1/2} \quad \text{(Eq. 2)}$$

where, I_p is the peak current in A. C is the concentration of the electroactive species (mol cm^{-3}), n is the number of electrons exchanged, D is the diffusion coefficient in $cm^2\ s^{-1}$, v is the scan rate ($V\ s^{-1}$) and A is the electroactive surface area (cm^2). The A was calculated to be 6.9 mm^2

Additionally, the amount of electroactive complex incorporated on the surface of the graphite paste electrode with S was calculated by using equation 3 (Eq.3).

$$I_p = n^2\ F^2A\Gamma\nu/4RT \quad \text{(Eq. 3)}$$

where, Γ (M/cm^2) is the surface coverage concentration, Ip is the peak current, and A are the scan rate and area of the working electrode respectively, n is the number of electrons exchanged, and R, F and T are physical constants with their usual meanings [38]. The Γ was calculated to be 2.05×10^{-7} M/cm^2

To investigate the effect of cations and anions from the supporting electrolytes on the voltammetric behavior of SZnH, several salts have been tested: KCl, NaCl, NH_4Cl, KNO_3, $NaNO_3$ and NH_4NO_3 (1.0 mol L^{-1}; ν = 20 mVs^{-1}), as illustrated in Figure 2 (A) and (B). The Table 1 below summarizes the principal parameters of these studies. The current intensities and the formal potentials ($E^{o'}$) were affected by the nature of the cations and anions, as shown in Figure 3 (A) and (B) Table 1. Furthermore, these studies indicated that the SZnH system formed a crystal lattice. SZnH has an analogous chemical structure to Prussian blue, exhibiting cavities that allow certain alkaline metal ions with smaller hydration radii to flow into and out of the crystal lattice.

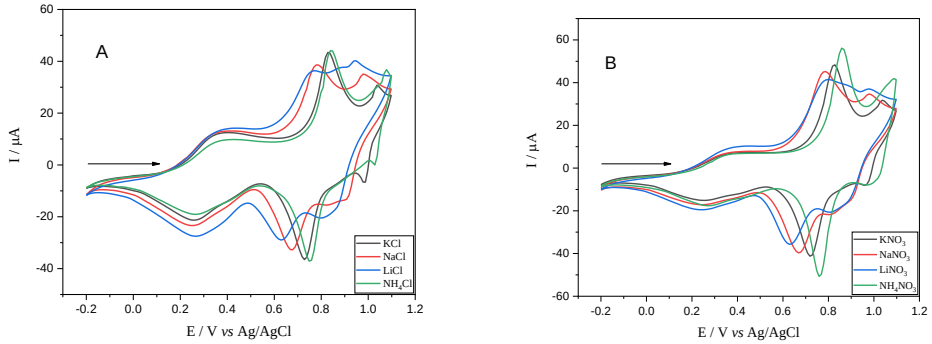

Figure 3. Cyclic voltammograms of the graphite paste electrode modified with SZnH and the presence of different electrolytes based on chlorides (A) and nitrates (B) (20% (m / m), 1.0 mol L^{-1}, *v*= 20 mV s^{-1}).

Table 1. Electrochemical parameters of graphite paste electrode with SZnH in different supporting electrolites (20% (m / m), 1.0 mol L^{-1}, ν= 20 mV s^{-1}).

Electrolite	Iap (µA)	Icp (µA)	|Iap/Ipc|	Eap (V)	Ecp (V)	$E^{\theta'}$ (V)	ΔEp (V)
KCl	33.11	-21.70	1.53	0.83	0.73	0.78	0.10
NaCl	26.58	-17.82	1.49	0.78	0.68	0.73	0.10
LiCl	22.52	-10.63	2.12	0.77	0.63	0.70	0.14
NH_4Cl	35.60	-21.44	1.66	0.84	0.75	0.80	0.09
KNO_3	41.27	-36.99	1.12	0.83	0.72	0.78	0.11
$NaNO_3$	37.64	-18.21	2.07	0.79	0.67	0.73	0.12
$LiNO_3$	31.10	-16.77	1.85	0.80	0.63	0.72	0.17
NH_4NO_3	49.25	-44.00	1.12	0.86	0.76	0.81	0.10

Figure 4 illustrates the cyclic voltammograms of graphite paste modified with SZnH at different concentrations of KCl (1.0×10^{-3} to 2.0 mol L^{-1}). It was observed that the voltammetric performance starts being different, with a decrease in current intensity and a shift of the average potential ($E^{\theta'}$) to more cathodic regions as the concentration of the supporting electrolyte decreases, indicating the effective participation of the cation K^+ in both redox processes.

Figure 4(B) illustrates the graph of the formal potential *vs* the log of the electrolyte concentration (K^+), for the second process, a linear relationship was observed, suggesting that the redox process II is highly dependent on the K^+ concentration. The slope of the line was 41 mV per decade of K^+ ion concentration, which is indicative of a *quasi*-Nernstian process [39], involving an electron.

To determine the slope of the above-mentioned straight line, only the voltammograms corresponding to concentrations from 0.01 to 2.0 mol L^{-1} were used, since below 0.01 mol L^{-1} the two redox processes are totally inhibited, as illustrated. the cyclic voltammogram for the electrode at a concentration of 0.001 mol L^{-1}. Table 2 lists the principal electrochemical parameters obtained from this study for the redox process II.

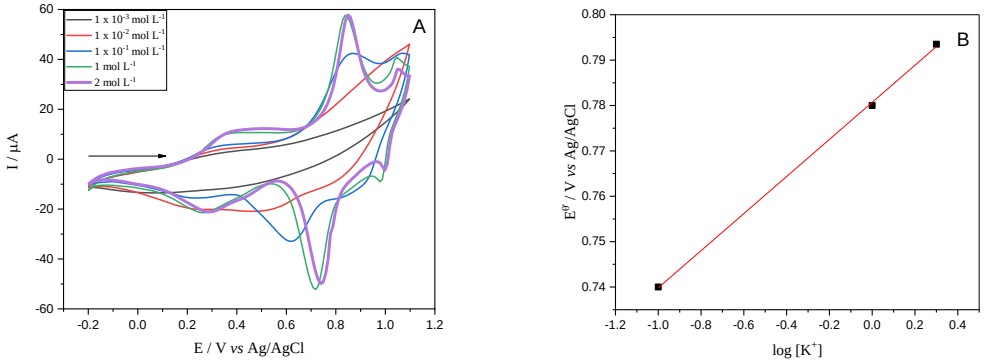

Figure 4. (A) Cyclic voltammogram of SZnH modified graphite paste at different concentrations of KCl. (B) The formal potential ($E^{\theta'}$) of graphite paste modified with SZnH as a functional of log of KCl concentration. (20% w/w, 1.0 mol L^{-1} KCl, v = 20 mV s^{-1}).

From the results obtained in this study, it is seen that the peak anodic (Iap) and cathodic (Icp) currents do not change too much when the concentration increases from 1.0 mol L^{-1} to 2.0 mol L^{-1} of the supporting electrolyte. Thus, the concentration of 1.0 mol L^{-1} of KCl was chosen.

Figure 5 shows the cyclic voltammograms obtained for SZnH at different hydrogenionic concentrations (pH 3.0 to 8.0). From these voltammograms, it can be observed that with increasing pH there is a slight increase in current intensity and a small shift from Eap and Ecp to more positive and more negative potentials, respectively. It was noted that the formal potential for the redox process II remained constant at 0.78 V. Since it is intended to study the electrocatalytic detection of drugs in biological mediums, the pH value chosen for subsequent testing was 7.0.

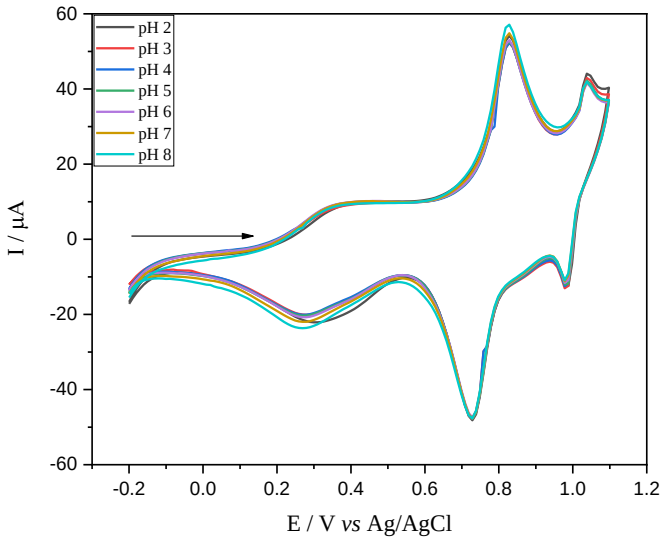

Figure 5. Cyclic voltammograms of the graphite paste electrode modified with SZnH at different pH (2-8) (KCl 1.0 mol L^{-1}, ν = 20 mV s^{-1}).

Figure 6 (A) illustrates the voltammetric behavior of SZnH at different scan rates (10 to 450 mV s^{-1}). It was observed for the redox process II that with the increase in scan rate there is an increase in the intensity of the anodic peak current (Ipa) and the $E^{\theta'}$ remained around 0.50 V, as shown in Figure 16 (A). The linear dependence between the anode peak current intensity and the square root of scan rate (inset graph (Fig. 6 (B)), which characterizes an adsorptive process for a "*quasi*" reversible system [40].

Based on the equations derived from Laviron [40], it was possible to find the electron transfer coefficient (α) as well as the charge transfer constant (ks). According to the Laviron Equation (Eq 4), $Ep\text{-}E^{\theta'}$ *vs* log *v* produces two straight lines with a gradient of *2.3RT/(1-α)nF* for anodic peak and *-2.3RT/αnF* for cathodic peak [41-43].

$$\log ks = \alpha\log(1-\alpha) + (1-\alpha)\log\alpha - \log \frac{RT}{(NFv)^{-1}} - \alpha nF(1-\alpha)\Delta Ep(2.3RT)^{-1} \qquad \text{(Eq. 4)}$$

In Figure 6 (C), plots of $E\text{-}E^{\theta'}$ *vs* log *v* are plotted, it is observed that starting from 10 mV s^{-1} there is a linear region (D) between $E\text{-}E^{\theta'}$ *vs* log *v* where the *2.3RT/(1-α)nF* for the anodic peak is *2.3RT/αnF* gives us the transfer coefficient (α) and using the Laviron equation (Eq. 4) it is possible to estimate the electron transfer rate (ks).

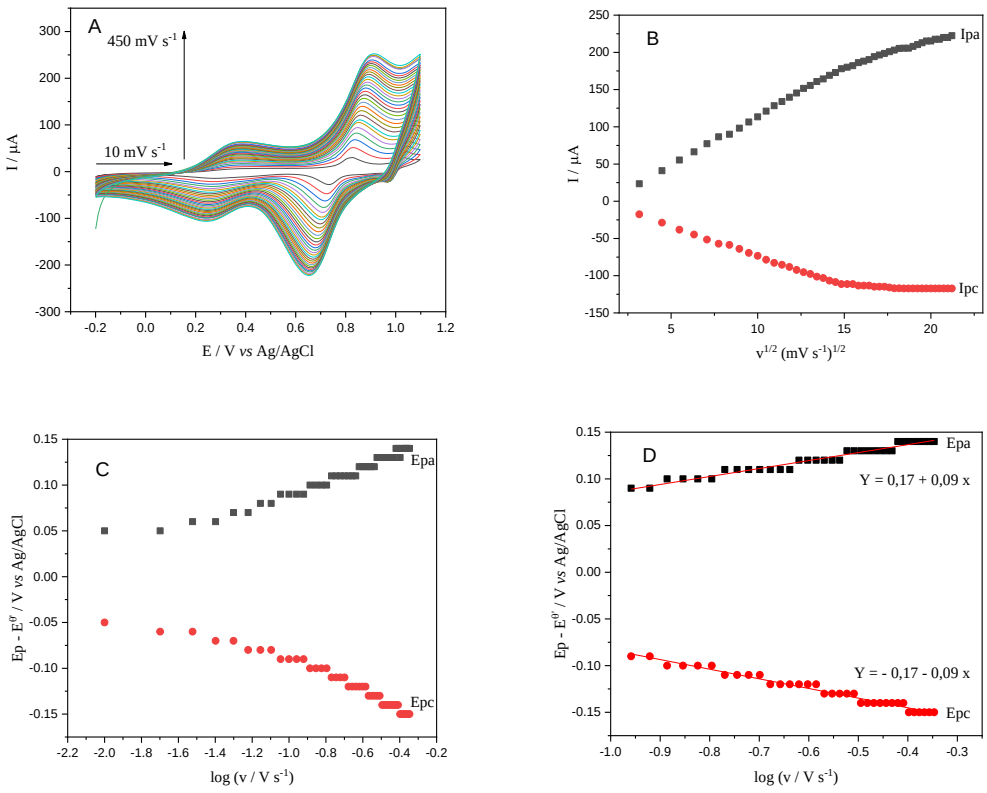

Figure 6. (A) Cyclic voltammograms of SZnH modified graphite paste at different scan rates 10 to 450 mV s^{-1} (20% w/w, KCl 1.0 mol L^{-1}). (B) Dependence of the current intensity of the anode and cathode peak (II) as a function of the scan rate. (C) Graph of Laviron, Epa and Epc *vs* log *v*. (D) Laviron Graph Line Equation, Epa and Epc *vs* log *v*.

Assuming that there is one electron involved in the redox process (Fe^{II}/Fe^{III}) and using the afore mentioned equations, α and *ks* can be determined to be equal to 0.69 for the anodic peak and 0.53 s^{-1}, respectively. Using the previously optimized electrochemical system, the catalytic properties of the graphite paste electrode with SZnH (GPSZnH) are evaluated by detecting 4-Chlorophenol (4-CP). The catalytic electro-oxidation of 4-CP on the SZnH-modified graphite paste electrode was studied using cyclic voltammetry, as shown in Figure 6. The graphite paste electrode did not present any redox pair on the scale of potential employed (-0.2 and 1.0 V) both in the absence (A) and in the presence of 7.0×10^{-5} mol L^{-1} of 4-CP (B), according to the results.

The electro-oxidation of 4-CP employing GPSZnH is showed in Figure 7, where the unmodified graphite paste electrode (GP) in the absence of 4-CP (A) didn't show any electrochemical signal in the potential range between -0.2 and 1.1 V, but, in the presence of 4-CP (b), an anodic peak at 0.89V corresponding to oxidation process 4-CP was observed. The GPSZn the absence of 4-CP (C) exhibited an anodic peak at 0.83 V, but, in the presence of 4-CP (D), an increase in current intensity of Ea_p (anodic peak potential) was observed. In general, the oxidation of 4-CP on the SZnH-modified paste electrode surface decreases the oxidation potential of 4-CP by approximately 60 mV, which is one characteristic of a catalytic electro-oxidation.

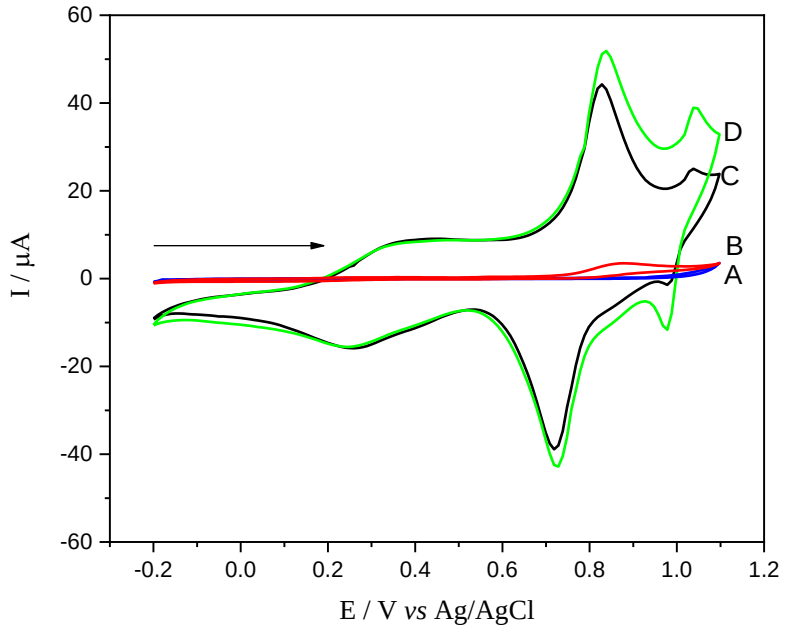

Figure 7. Cyclic voltammograms of: (A) only graphite paste electrode, (B) graphite paste electrode in the presence of 6.0×10^{-5} mol L^{-1} of 4-CP, (C) SZnH graphite paste electrode in the absence of 4-CP and (D) SZnH-modified graphite paste electrode in the presence of 6.0×10^{-5} mol L^{-1} of 4-CP (20% w/w; 1.0 mol L^{-1} KCl ; pH 7.0; ν = 20mV s^{-1}).

Figure 8 (A) shows the voltammetric behavior of the SZnH system after additions of different aliquots of 4-CP. The analytic curve, showing the anodic current as a function of 4-CP concentration for SZnH is illustrated in Figure 8 (B). The modified graphite paste electrode showed a linear response in

the concentration range of 6.0×10^{-7} to 6.0×10^{-5} mol L^{-1}, presented a corresponding equation Y (μA) = 40.10 + 5.3 × 10^5 [4-CP] Y and a correlation coefficient r = 0.997. The detection limit obtained for this system was of 5.3 $\times10^{-6}$ with a relative standard deviation of ± 1.7% (n = 3) and an amperometric sensitivity of 0.53 A/mol L^{-1}. The Table 2, shows other additional electrochemical parameters of SZnH modified graphite paste electrode used for 4-CP electrooxidation.

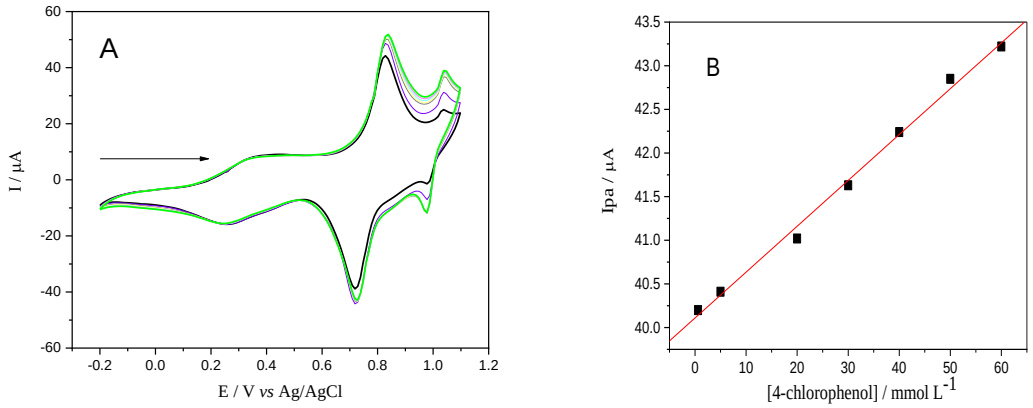

Figure 8. Cyclic voltammograms for the SZnH-modified graphite paste: **(A)** at different 4-CP concentrations (6.0×10^{-7} to 6.0×10^{-5} mol L^{-1}); **(B)** analytical curve of the anodic peak for 4-CP determination (20% w/w; 1.0 mol L^{-1} KNO_3; pH 7.0; ν = 20mV s^{-1}).

Table 2. Main electrochemical parameters of SZnH modified graphite paste electrode used for 4-CP electrooxidation.

Electroanalytical Parameters	Numerical data
Concentration range (mol L^{-1})	6.0×10^{-7} to 6.0×10^{-5} mol L^{-1}
Corresponding Equation	Y (μA) = 40.10 + 5.3 × 10^5 [4-CP]
Correlation Coefficient (r)	0.997
Limit of Detection (LOD) mol L^{-1}	5.3 $\times10^{-6}$
Limit of Quantification (LOQ) (mol L^{-1})	1.75×10^{-5}
Standard deviation	± 1.7% (n = 3)
Amperometric Sensitivity (A/mol L^{-1})	0.53

The graphite paste electrode modified with ACZnN obtained satisfactory results, compared to others described in the literature [44-49], as shown in Table 3, where different electrochemical techniques are used in the determination of 4-CP.

Table 3. Analytical parameters for the electrocatalytic detection of 4-CP using different modified electrodes and voltammetric techniques described in the literature.

Techniques *	Electrodes	Concentration range (μmol L^{-1})	Limit of detection (μmol L^{-1})	References
CV	Nafion/CNT	1-25	12.09	44
MPA	graphite-epoxy composite (EG-Epoxy)	100 -500	10.0	45
LSV	EG-Epoxy electrode	80-1000	20	46
DPV	HRP/PCRG/GCE	1-800	15.2	47
CV	PVAc/F108d/AuNPs/ Lac GCE	1-25	12	48
CV	CNTs-OH/PtNPs/RhB/GCE	10–300	3.69	49
CV	Graphite paste SZnH	0.6-60	5.3	This paper

*CV= Cyclic Voltammetry; *MPA*= multiple pulsed amperometry*;* LSV = Linear Scan Voltammetry. DPV= Differential Pulse Voltammetry

The interference study was conducted considering the possible application of the sensor in analysis of tape water supply samples, where the main interfering agents are ionic species such as sodium, calcium, magnesium and ammonium salts and that are usually present in a mixture. Thus, the interfering study was carried out using a mixed solution. Table 4 shows the relative responses (%) obtained in the presence of a mixed solution containing the afore mentioned interfering species. According to the voltammograms presented, the interferents practically do not affect the SZnH current response in the presence of only 4-CP and with the addition of the interferents, the signals change only <2% (Fig. 9d). Thus, the good performance of the presented sensor and good selectivity suggest that the sensor may be viable for detecting 4-CP in supply water.

It is crucial to be able to quantify the concentration of 4-CP in solutions because it is very toxic and causes a variety of diseases. Because of that, it is important to develop a rapid, low cost and efficient sensor that can measure the concentration of 4-CP in solutions. Utilizing the CV technique, a SZnH graphite paste electrode was used to determine 4-CP in tap water samples by the standard addition method. The spike/recovery test for the tap water was done by adding appropriate aliquots of standard 4-CP solutions to real samples. The recovery values, in Table 5, are in satisfactory range (87 to 110 %), corroborating that the SZnH graphite paste electrode for determination of 4-CP in tap water is a good feasible method.

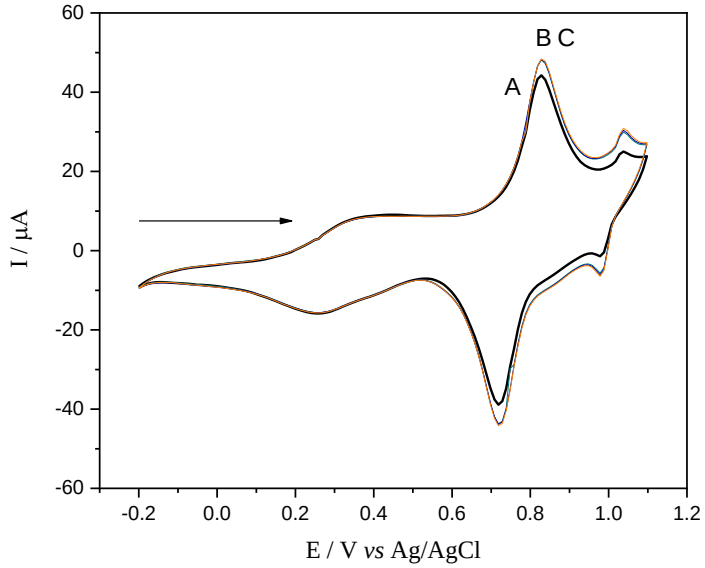

Figure 9. Cyclic voltammograms for the GPSZnH: in absence of 4-CP (a); in presence of 41 µmol L^{-1} 4-CP (B); and after addition of 410 µmol L^{-1} of interferes mixture solution (C) (20 % w/w; KCl 2.0 mol L^{-1}, pH 7.0, v = 20 mVs^{-1}).

Table 4. Interference effect of foreign ionic species in the voltammetric determination of 4- CP (41 µmol L^{-1}).

Interferes	Concentration (µmol L^{-1})	Interference percentage (%)
NH_4Cl + NaCl, $CaCl_2$ + $MgCl_2$	41	0.7
NH_4Cl + NaCl, $CaCl_2$ + $MgCl_2$	410	1.6

The spiked water samples were prepared by adding known concentrations of 4-CP solution to water tap samples. Table 5 presents the recovery of 4-CP and its relative standard deviation. Taking into account the excellent sample recovery, the proposed sensor can efficiently detect the presence of 4-CP in tap water.

Table 5. Recoveries of 4-CP and in tape water samples using Voltammetric method at modified graphite paste electrode.

Spiked concentration (µmol L^{-1})	Found concentration (µmol L^{-1})	Recovery (%)
0.2	0.17	85
0.4	0.44	110
0.6	0.57	95
0.8	0.84	105
10.0	0.97	97

4. CONCLUSIONS

The nanostructured material showed a well-defined three redox couples with formal potential ($E^{\theta'}$) of approximately 0.33, 0.78 and 1.01 ± 0.01V (*vs* Ag/AgCl). Through voltammetric study it was possible to check that formal potential ($E^{\theta'}$) is strong influenced by concentration and electrolyte nature, but the system remained unchanged at pH values between 2 and 8. The SZnH graphite paste electrode modified presented a sensitive and catalytic oxidation response for the determination of 4-CP. The modified graphite paste electrode achieved a linear range from 6.0×10^{-7} to 6.0×10^{-5} mol L^{-1} with limit of detection 5.3×10^{-6} mol L^{-1} and amperometric sensitivity of 0.53 A/ mol L^{-1} in the 4-CP detection. This electrode could be used in detection of 4-CP in tap water.

ACKNOWLEDGMENTS
The authors wish to thank the Fundação de Amparo à Pesquisa do Estado de São Paulo (FAPESP-Process 2015/20397-8) and the Coordenação de Aperfeiçoamento de Pessoal de Nível Superior (CAPES) for their financial support.

References

1. RH. Baney, M. Itoh, A. Sakakibara and T. Suzuki. *Chemical Reviews*, 95 (1995) 1409.
2. A. Provatas and J.G. Matisons, *Trends in polymer science*, 5 (1997) 327.
3. F.J. Feher, D.A. Newman and J.F. Walzer. *Journal of the American Chemical Society*, 111 (1989) 1741.
4. F.J. Feher, T.A. Budzichowski, R.L. Blanski, K.J. Weller and J.W. Ziller, *Organometallics*, 10 (1991) 2526.
5. A.R. Bassindale, M. Pourny, P.G. Taylor, M.B. Hursthouse and M.E. Light, *Angewandte Chemie*, 115 (2003) 3612.
6. J.D. Lichtenhan, *Comments on Inorganic chemistry*, 17 (1995) 115.
7. J.D. Lichtenhan, *Polymeric materials encyclopedia* 10 (1996) 7768.
8. J.D. Lichtenhan, N.Q. Vu, J.A. Carter, J.W. Gilman and F.J. Feher, *Macromolecules*, 26 (1993) 2141.
9. S. Sulaiman, M. Ronchi, J. H. Jung and R. M. Laine, Unpublished work.
10. S.G. Kim, S. Sulaiman, D. Fargier and R.M. Laine, *Materials Syntheses* (2008) 179.
11. P.P. Pescarmona and T. Maschmeyer, *Australian journal of chemistry*, 54 (2002) 583.
12. D.R. Do Carmo, P.F.P. Barbosa and L.R. Cumba, *Silicon*, 12 (2020) 1111.
13. D.R. do Carmo, N.L.D. Filho and N.R. Stradiotto, *Materials Research Bulletin*, 42 (2007) 1811.
14. T. W.J.M. Hanssen, A.V.S. Rutger and H.C.L. Abbenhuis, *European Journal of Inorganic Chemistry*, 4 (2004) 675.
15. D.M.L. Goodgame, S. Kealey, P.D. Lickiss and A.J.P. White. *Journal of Molecular Structure* 890 (2008) 232.
16. S. Sharma, M. Mukhopadhyay and Z.V.P. Murthy, *Industrial & engineering chemistry research* 49 (2010) 3094.
17. C. Merriman, D.H. Anthony, J.A. Kraft, and R.J. Wilkinson, *Chemosphere*, 23 (1991) 1605.
18. N.K. Kristiansen, M. Froshaug, K.T. Aune, G. Becher and E. Lundanes, *Environmental science & technology* 28 (1994) 1669.
19. M. Nazari, S. Kashanian and R. Rafipour, *Spectrochim. Acta A* 145 (2015) 130.
20. K.D. Wang, P.S. Chen and S.D. Huang, *Analytical and bioanalytical chemistry*, 406 (2013) 2123.
21. R. Alizadeh, *Talanta*,146 (2016) 831.

22. Y. Zhang, J. Zhang, H. Wu, S. Guo and J. Zhang, *Journal of Electroanalytical Chemistry*, 681 (2012) 49.
23. J. Zolgharnein, T. Shariatmanesh, A. Babaei, *Sensors and Actuators B: Chemical* 186 (2013) 536.
24. L. Xu, S. Ling, H. Li, P. Yan, J. Xia, J. Qiu, K. Wang and S. Yuan, *Sensors and Actuators B: Chemical*, 240 (2016) 308.
25. J. Liu, J. Niu, L. Yin and F. Jiang, *Analyst*, 136 (2011) 4802.
26. B. Wang, O. K. Okoth, K. Yan and J. Zhang. *Sensors and Actuators B: Chemical*, 239 (2016) 294.
27. C. Qiu, T. Chen, X. Wang, Y. Li and H. Ma, *Colloids and Surfaces B: Biointerfaces*, 103 (2013) 129.
28. F. Pino, C.C. Mayorga-Martinez and A. Merkoçi, *Electrochemistry Communications*, 71 (2016) 33.
29. A. Bebeselea, F. Manea, G. Burtica, L. Nagy and G. Nagy, *Talanta*, 80 (2010) 1068.
30. L. Wang, Q. Sun, Y. Liu and Z. Lu, *RSC advances* 6 (2016) 34692.
31. A. Khursheed and M.M. Shaikh, *Nanoescale advances*, 1 (2019) 719.
32. F.J. Feher, K.D. Wyndham and D. Soulivong, F. Nguyen, *Journal Of The Chemical Society*, (1999) 1491.
33. W.J. Wang, X. Hai, Q.X. Mao, M.L. Chen and J.H Wang, *ACS Applied Materials & Interfaces*, 30 (2015) 16609.
34. Z. Bahrami, A. Akbari and B. Eftekhari-Sis, International *journal of biological macromolecules*, 129 (2019) 187.
35. J. Rodríguez-Hernández, E. Reguera, E. Lima, J. Balmaseda, R. Martínez-García and H. Yee-Madeira, *Journal of Physics and Chemistry of Solids*, 68 (2007) 1630.
36. K. Nakamoto, Infrared and Raman Spectra of Inorganic and Coordination Complexes Wiley (1986) New York.
37. A.A. Kumar, B.K. Swamy, T.S. Rani, P.S. Ganesh and Y.P. Raj, *Materials Science and Engineering*, 98 (2019) 746.
38. P. S. Ganesh, G. Shimoga, S. H. Lee, S.Y. Kim and E.E. Ebenso, *Chemistry Select*, 6 (2021) 2379.
39. D. Engel and E.W. Grabner, *Berichte der Bunsengesellschaft für physikalische Chemie*, 89 (1985) 982.
40. A.J. Bard and L.R. Faulkner, Electrochemical Methods Fundamentals and Applications, (2001) New York.
41. E. Laviron, *Journal of Electroanalytical Chemistry and Interfacial Electrochemistry*, 101 (1979) 19.
42. R. Ojani, J.B. Raoof and B. Norouzi, *Electroanalysis: An International Journal Devoted to Fundamental and Practical Aspects of Electroanalysis*, 20 (2008) 1996.
43. Y. Liu and L. Xu, *Sensors*, 7 (2007) 2446.
44. A. S. Arribas, M. Moreno, E. Bermejo, J. A. Pérez, V. Román, A. Zapardiel, and M. Chicharro, *Electroanalysis*, 23 (2011) 237.
45. A. Bebeselea, F. Manea, G. Burtica, L. Nagy and G. Nagy, *Talanta*, 80 (2010) 1068.
46. A. Pop, F. Manea, C. Radovan, I. Corb, G. Burtica, P. Malchev, S.J. Picken and J. Schoonman, *Rev. Roum. Chim*, 53 (2008) 623.
47. Y. Zhang, J. Zhang, H. Wu, S. Guo and J. Zhang, *Journal of Electroanalytical Chemistry*, 681 (2012) 49.
48. J. Liu, J. Niu, L. Yin and F. Jiang, *The Analyst*, 136 (2011) 4802.
49. X. Zhu, K. Zhang, D. Wang, D. Zhang, X. Yuan and J. Qu, *Journal of Electroanalytical Chemistry*, 810 (2018) 199.

© 2022 The Authors. Published by ESG (www.electrochemsci.org). This article is an open access article distributed under the terms and conditions of the Creative Commons Attribution license (http://creativecommons.org/licenses/by/4.0/).